Electronic Supplementary Material (ESI) for Journal of Materials Chemistry A.
This journal is © The Royal Society of Chemistry 2019

Supporting Information

Graphene Oxide Membranes with Ultra-Large Interlayer Distance through Vertically Grown Covalent Organic Framework Nanosheets

Yanan Liu[a,b], Jingyuan Guan[a,b], Yanlei Su[a,b], Runnan Zhang[a,b], Jialin Cao[a,b], Mingrui He[a,b], Jinqiu Yuan[a,b], Fei Wang[a,b], Xinda You[a,b] , Zhongyi Jiang[a,b*]*

a Key Laboratory for Green Chemical Technology of Ministry of Education, School of Chemical Engineering and Technology, Tianjin University, Tianjin 300072, China

b Collaborative Innovation Center of Chemical Science and Engineering (Tianjin), Tianjin 300072, China

∗ Corresponding author. School of Chemical Engineering and Technology, Tianjin University, No. 92, Weijin Road, Nankai District, Tianjin 300072, China

Tel: 86-22-27406646. Fax: 86-22-23500086.

E-mail address: runnan.zhang@tju.edu.cn; zhyjiang@tju.edu.cn

1. Table of membrane abbreviations and their preparation conditions

Table S1. Membrane abbreviations and their preparation conditions

Membrane	Mass of GO (μg)	Mass of v-COF@GO (μg)	Mass ratio of GO in v-COF@GO (%)
GO	20	0	0
GO/v-COF@GO-1	20	106	18.79
GO/v-COF@GO-2	20	123	16.20
GO/v-COF@GO-3	20	153	13.09
GO/v-COF@GO-4	20	191	10.45
GO/v-COF@GO-5	20	238	8.39
GO/v-COF@GO-6	20	306	6.53

2. The particle size distribution of surfactant-stabilized oil-in-water emulsions including pump oil-in-water emulsion, silicone oil-in-water emulsion, soybean oil-in-water emulsion and hexadecane-in-water emulsion

Four kinds of oil-in-water emulsions were employed: 1.0 g pump oil, silicone oil, soybean oil or hexadecane and 0.1 g sodium dodecyl sulfate were added into 1000 mL ultrapure water, and then mechanically stirred for more than 12 h. Four kinds of emulsions possessed similar mean particle size which were 255 nm, 227 nm, 238 nm and 232 nm for pump oil-in-water emulsion, silicone oil-in-water emulsion, soybean oil-in-water emulsion and hexadecane-in-water emulsion, respectively.

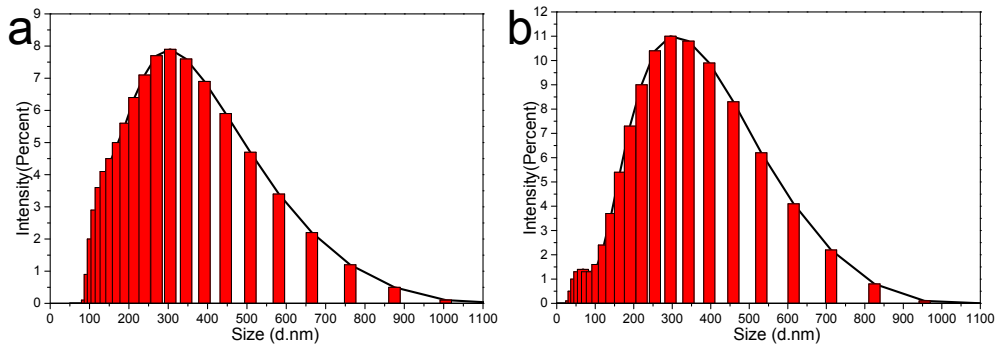

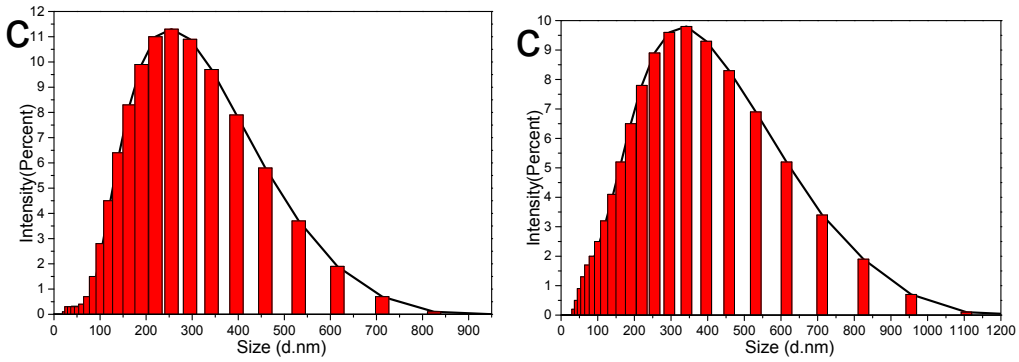

Fig. S1. The particle size distribution of surfactant-stabilized oil-in-water emulsions including a) pump oil-in-water emulsion, b) silicone oil-in-water emulsion, c) soybean oil-in-water emulsion and d) hexadecane-in-water emulsion.

3. AFM, TEM images and FTIR of GO nanosheets

The GO nanosheets utilized in this study were commercial products with 0.8 nm thickness and 7 μm size, and possessed hydroxyl, epoxy, carboxyl and carbonyl groups, which were demonstrated by the results of AFM, TEM images and FTIR of GO nanosheets.

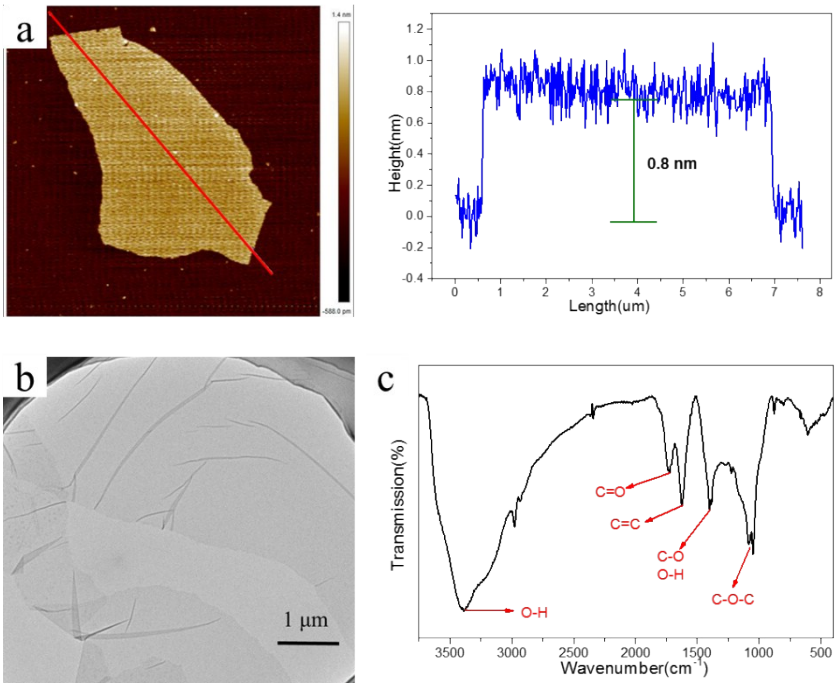

Fig. S2. a) AFM images, b) TEM images and c) FTIR of GO nanosheets

4. The water contact angles of v-COF@GO nanoheterojunctions before and after sulfonation.

Before the measurement of water contact angle, v-COF@GO nanoheterojunctions were

compressed into a slice. And then the water contact angle of v-COF@GO nanoheterojunctions was measured by testing the water contact angle of v-COF@GO nanoheterojunctions slice. The water contact angles of v-COF@GO nanoheterojunctions before and after sulfonation were 64.3±3.6^{o} and 36.2±2.9^{o}, respectively, which demonstrated that sulfonation could increase the hydrophilicity of v-COF@GO nanoheterojunctions.

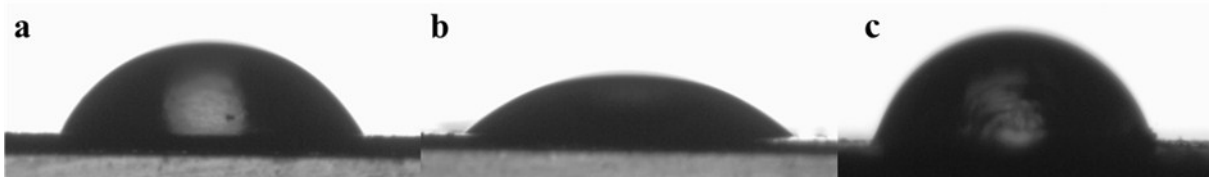

Fig. S3. The water contact angle of v-COF@GO nanoheterojunctions a) before, b) after sulfonation and c) water contact angle of GO membrane

5. SEM images of v-COF@GO nanoheterojunctions with different loadings of COFs nanosheets on GO nanosheets.

By varying the mass ratio of GO nanosheets to amino and aldehyde monomers, a series of 2D/2D v-COF@GO nanoheterojunctions with different COFs size were synthesized. With the decrease of GO nanosheets mass, the COFs nanosheets on the surface of GO nanosheetss became bigger

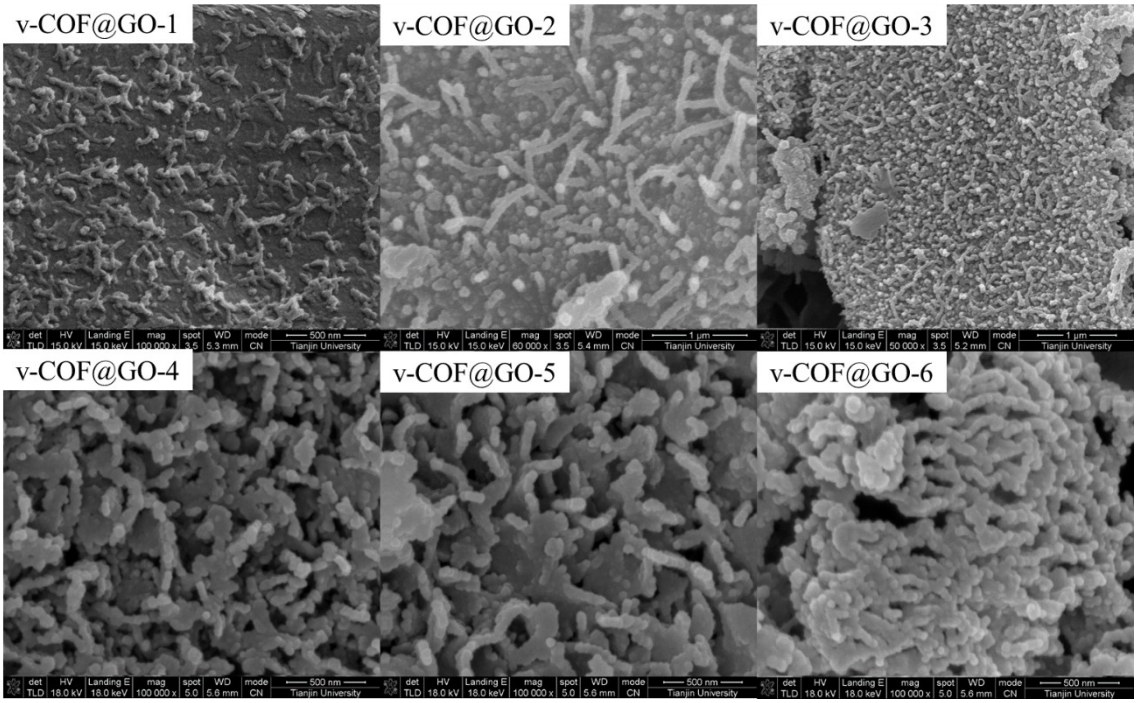

Fig. S4. SEM images of v-COF@GO nanohetrojunctions with different loadings of COFs nanosheets on GO nanosheets

6. AFM image of v-COF@GO-5 nanoheterojunction.

The v-COF@GO-5 nanoheterojunction possessed the most ideal structure, and the thickness and size of v-COF@GO-5 nanoheterojunctions were 7 μm and 498 nm, respectively.

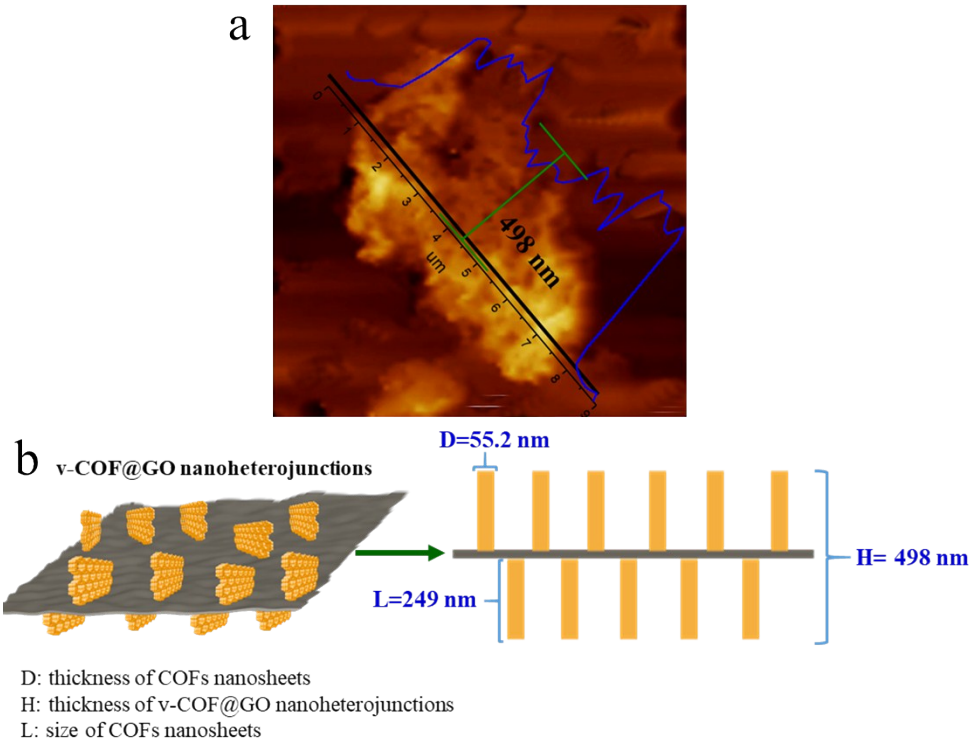

Fig. S5. a) AFM image and b) schematic diagram of v-COF@GO-5 nanoheterojunction

7. FTIR of v-COF@GO nanohetrojunctions with different loadings of COFs nanosheets on GO nanosheets

The FTIR spectra exhibited that v-COF@GO nanohetrojunctions possessed similar chemical structure, and typical peaks of COFs including carbonyl (C=O) peak and newly formed C=C bond at 1610 cm^{-1} and 1589 cm^{-1}, respectively.

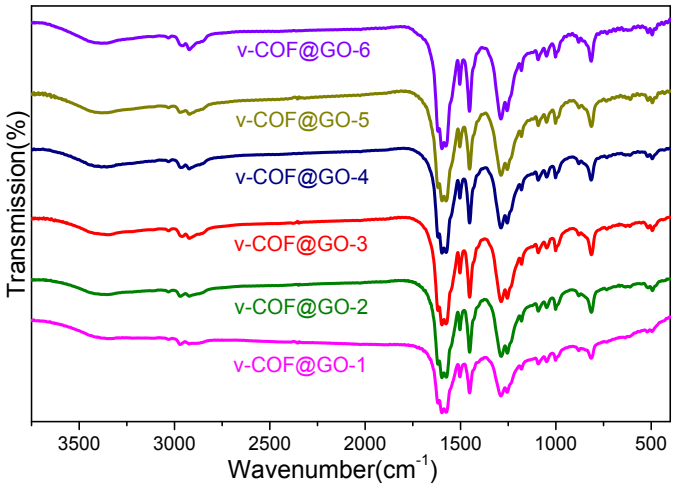

Fig. S6. FTIR of v-COF@GO nanohetrojunctions with different loadings of COFs nanosheets on GO nanosheets

8. ^{13}C NMR of v-COF@GO nanoheterojunctions before and after sulfonation.

^{13}C NMR of v-COF@GO nanoheterojunctions before and after sulfonation was measured, and a new park at 134.4 ppm appeared, demonstrating sulfonic acid group on v-COF@GO nanoheterojunctions.

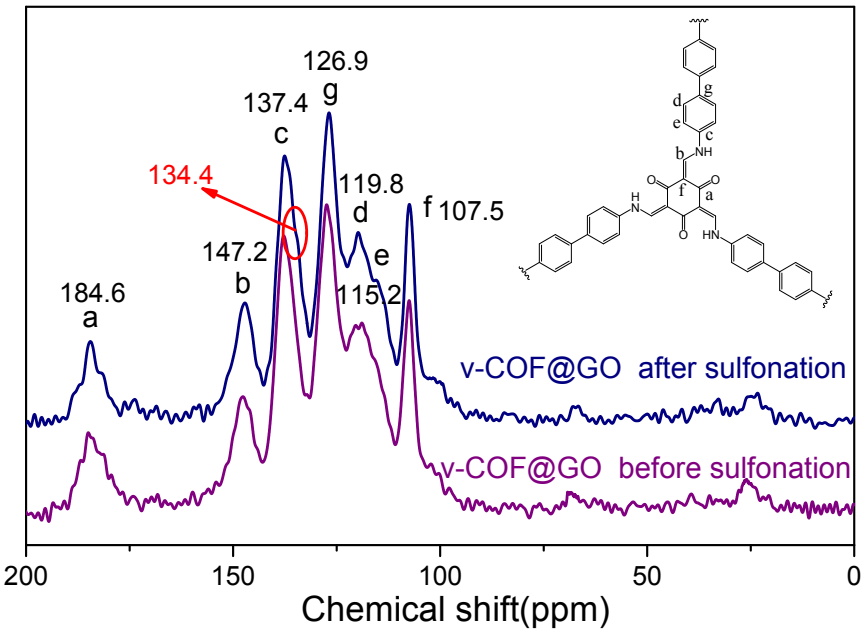

Fig. S7. ^{13}C NMR of v-COF@GO nanoheterojunctions before and after sulfonation.

9. XRD of GO/v-COF@GO membranes

The crystallinity of COFs after membrane the GO/v-COF@GO membranes fabrication

process, which demonstrated the integrity of the COFs structure after membrane fabrication process.

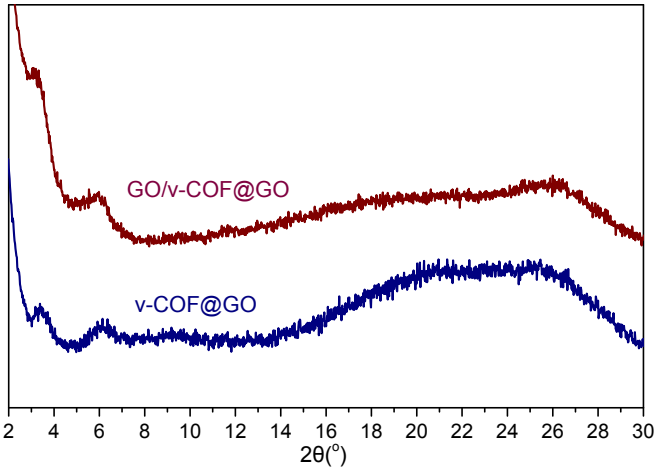

Fig. S8. XRD of GO/v-COF@GO membranes and v-COF@GO nanoheterojunctions

10. SEM and AFM images of GO membrane

GO membrane exhibited a quite smooth surface with slightly wrinkled corrugation.

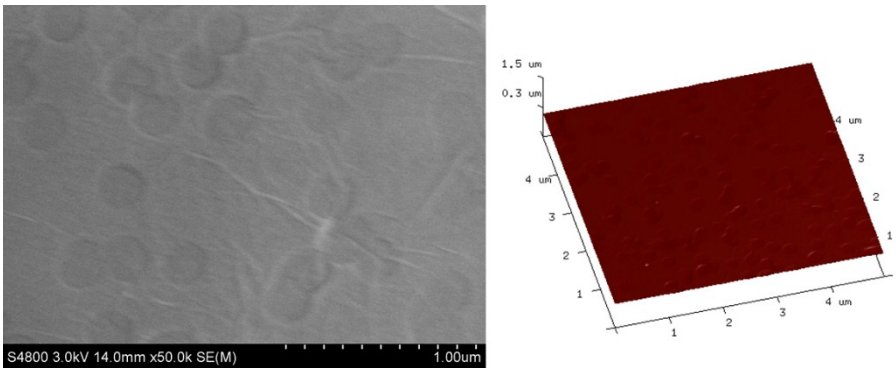

Fig. S9. SEM and AFM images of GO membrane

11. Surface roughness parameters of GO/v-COF@GO membranes

After intercalating the v-COF@GO nanoheterojunctions, the GO/v-COF@GO membrane exhibited a rough surface, and when the mass of COFs nanosheets on v-COF@GO nanoheterojunctions increased, the surface of GO/v-COF@GO membranes became rougher. Because strong interaction between COFs nanosheets and GO nanosheets made GO nanosheets more flat and inflexible, and easier to form embossment than flexible nanosheets. Hence, the surface roughness parameter Ra of GO/v-COF@GO membranes was increased from 6.0±1.3

nm of GO membrane to 171.0±34.6 nm of GO/v-COF@GO-6 membrane, and surface roughness parameter Rq was increased from 10.5±2.8 nm of GO membrane to 218.2±50.2 nm of GO/v-COF@GO-6 membrane

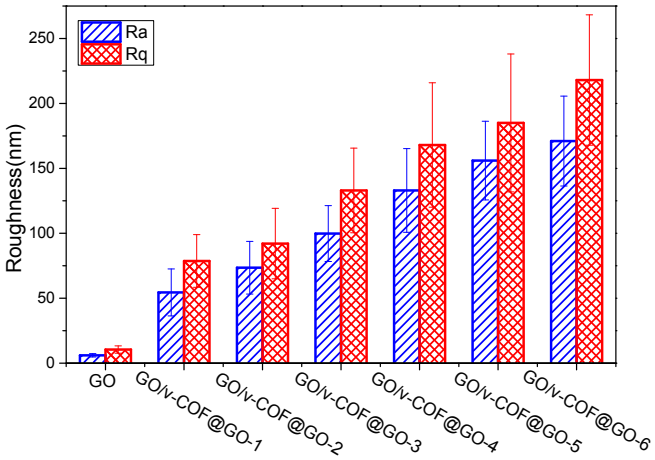

Fig. S10. Surface roughness parameters of GO/v-COF@GO membranes

12. XRD pattern of GO membrane

For GO-based membranes, the interlayer spacing between GO nanosheets acted as mass transfer channels for selective permeation and was of variable size. And the GO membrane exhibited the interlayer spacing of 0.81 nm, which was evaluated by XRD with diffraction peak of 2θ=10.9°

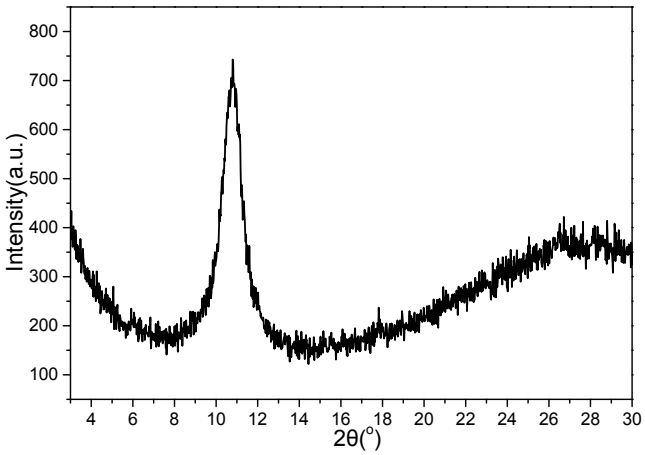

Fig. S11. XRD pattern of GO membrane

13. Comparison of the permeability of the membranes with that of the state-of-the-art GO-based membranes in the literature

Compared with GO-based membranes made from other intercalation materials, GO/v-COF@GO membranes possessed ultra-large interlayer spacing for water transport.

Table S1. Comparison of the permeability of the membranes with that of the state-of-the-art GO-based membranes in the literature

Membranes	Intercalation materials	Interlayer spacing (nm)	Permeability	Application	References
GO/v-COF@GO	v-COF@GO	0.81-42.2	10967 $Lm^{-2}h^{-1}bar^{-1}$	Oil/water separation	This work
GO	-	0.9-1.31	0.2 $Lm^{-2}h^{-1}$	Ion sieving	1
B-GO	Borate	0.68-0.79	650 GPU	Gas separation	2
GOM	Cations	1.21-1.36	0.36 $Lm^{-2}h^{-1}$	Ion sieving	3
GO-poly(VPA-co-EGDMA)	Poly(phosphonic acid)	~1.43	-	Proton conduction	4
GO-RF8	Octapeptide	0.870-1.624	716 $Lm^{-2}h^{-1}bar^{-1}$	Dyes separation	5
GOT	TiO_2 nanoparticles	-	75 $Lm^{-2}h^{-1}bar^{-1}$	Dyes separation	6
NSC-GO	Copper hydroxide nanostrands	-	695 $Lm^{-2}h^{-1}bar^{-1}$	Dyes separation	7
SWCNT-intercalated GO	Single-walled carbon nanotube	0.789-0.823	720 $Lm^{-2}h^{-1}bar^{-1}$	Dyes separation	8
GO/g-C_3N_4@TiO_2	g-C_3N_4@TiO_2	0.81-5.62	4536 $Lm^{-2}h^{-1}bar^{-1}$	Oil/water separation	9

14. TEM images of GO/v-COF@GO membrane

The TEM results showed that the interlayer distance between GO nanosheets was not uniform,

which was in the range of several nanometers to tens nanometers.

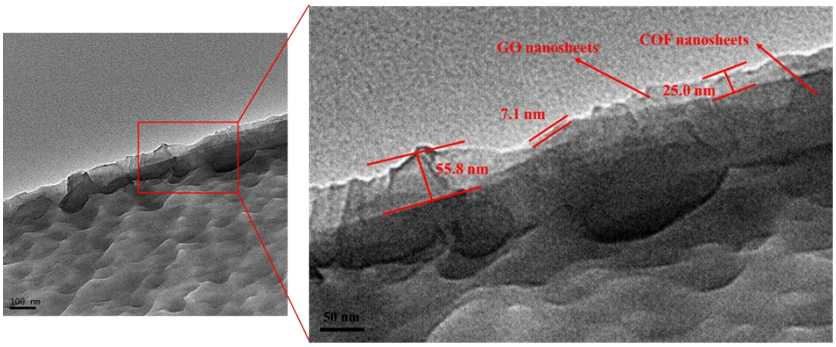

Fig. S12. TEM images of GO/v-COF@GO membrane

15. The morphology and thickness of GO/COF membrane as well as the permeate flux of GO/COF membranes under different applied transmembrane pressure

The GO/COF membranes were prepared *via* the uniform procedure with GO/v-COF@GO membrane by intercalating pure COFs with the same mass as v-COF@GO-5 nanoheterojunction. The thickness of GO/COF membranes was 459.4±53.2 nm, and the surface roughness of GO/COF membrane were 44.5±14,8 nm and 64.5±22.3 nm for Ra and Rq, respectively. The water permeability of the GO/COF membrane increased with the increase of the applied transmembrane pressure. Nevertheless, the water permeability coefficient was decreased with the increase of the applied pressure, demonstrating that the interlayer spacing of GO nanosheets in GO/COF membrane was compressed by the pressure, giving rise to the increase of mass-transfer resistance.

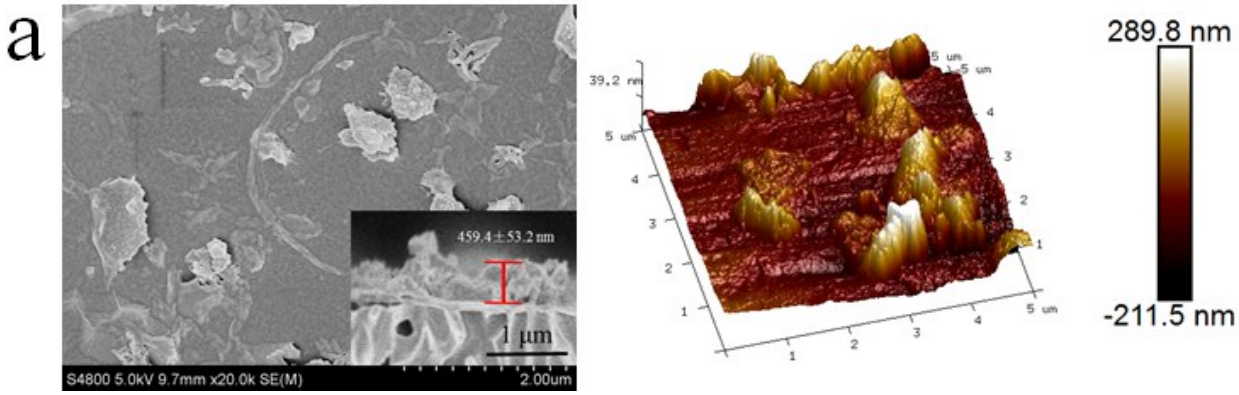

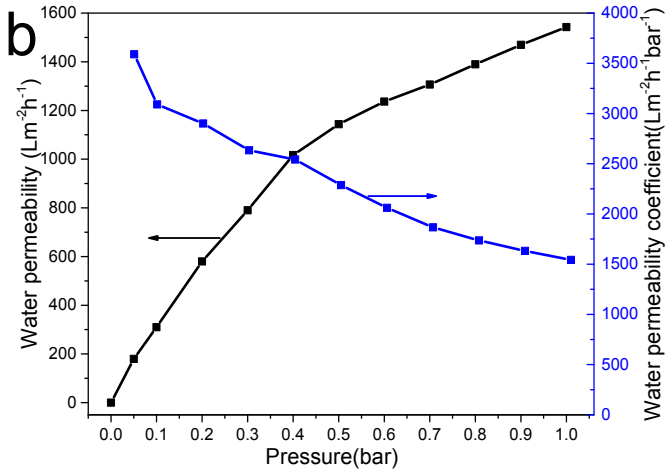

Fig. S13. a) The morphology and thickness of GO/COF membrane, b) the permeate flux of GO/COF membranes under different applied transmembrane pressure

16. Permeate flux of GO/v-COF@GO membranes at different pHs

The permeate flux of GO/v-COF@GO membrane was stable in the pH range of 3.0-11.0. These results illustrated the structural stability of GO/v-COF@GO membranes.

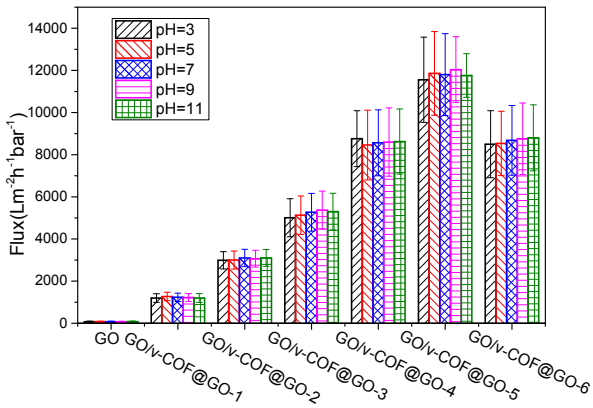

Fig. S14. Permeate flux of GO/v-COF@GO membranes at different pHs

17. The morphology and thickness of GO/v-COF@GO membrane after immersing in water for 2 months

For GO/v-COF@GO membrane, there was interaction between carboxyl groups on GO nanosheets and amino groups on COFs nanosheets, which would link v-COF@GO nanoheterojunctions and GO nanosheets to avoid swelling in water and keep intact structure of as-prepared membrane. Hence, after immersing in water for two months, the GO/v-COF@GO

membrane exhibited similar structure with the non-immersed membrane, including unchanged appearance, morphology and thickness The surface morphology of GO/v-COF@GO membrane after immersing in water for 2 months was measured by SEM and AFM images, which showed a rough surface with surface roughness parameters Ra of 151.3±29.5 nm and Rq of 197.7±54.3, and the thickness of GO/v-COF@GO membrane after immersing in water for 2 months was 2.4±0.2 μm, which was in similar with the surface morphology and thickness of GO/v-COF@GO membrane before immersing in water for 2 months.

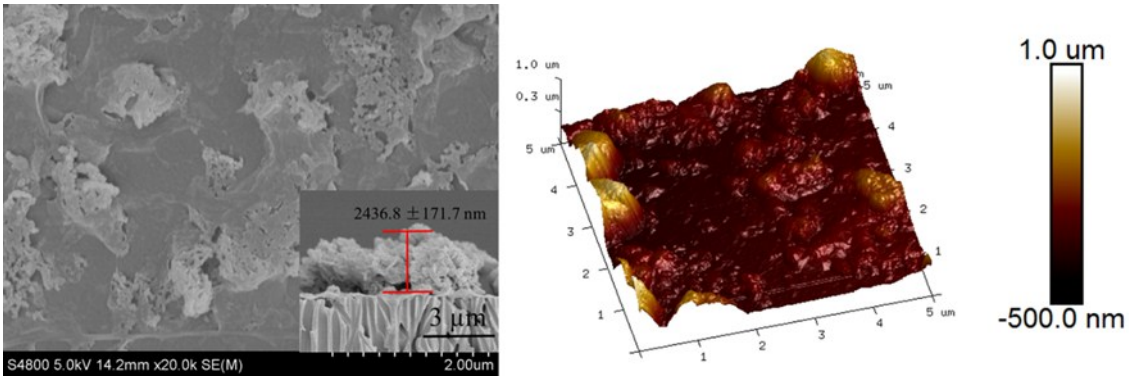

Fig. S15. SEM and AFM images of GO/v-COF@GO membrane after immersing in water for 2 months

18. Dynamic approach-compress-detach oil-adhesion process of GO/v-COF@GO membranes

The underwater oil-adhesion test of GO/v-COF@GO membranes was investigated *via* an approach−compress−detach process. Oil droplets of 10 μL were trapped on the needle tip of a microsyringe and forced to be in contact the membranes. As the oil droplets were compressed on membrane surfaces, oil droplets were deformed from a spherical to ellipsoidal form. When an oil droplet was removed downward, the adhesion force between the oil droplet and membrane surface generated vertical tensile stress and promoted the deformation. As the oil droplets were removed downward, oil droplets could overcome the adhesion force with membrane surfaces and detach from membrane surfaces. Particularly, almost no obvious deformation was found when the oil droplet detached from the GO/v-COF@GO membrane

surface, and the oil droplet deformed obviously and kept on GO membrane surface when oil droplet detached from GO membrane surface, which revealed lower oil-adhesiveness of the GO/v-COF@GO membrane than that of GO membrane.

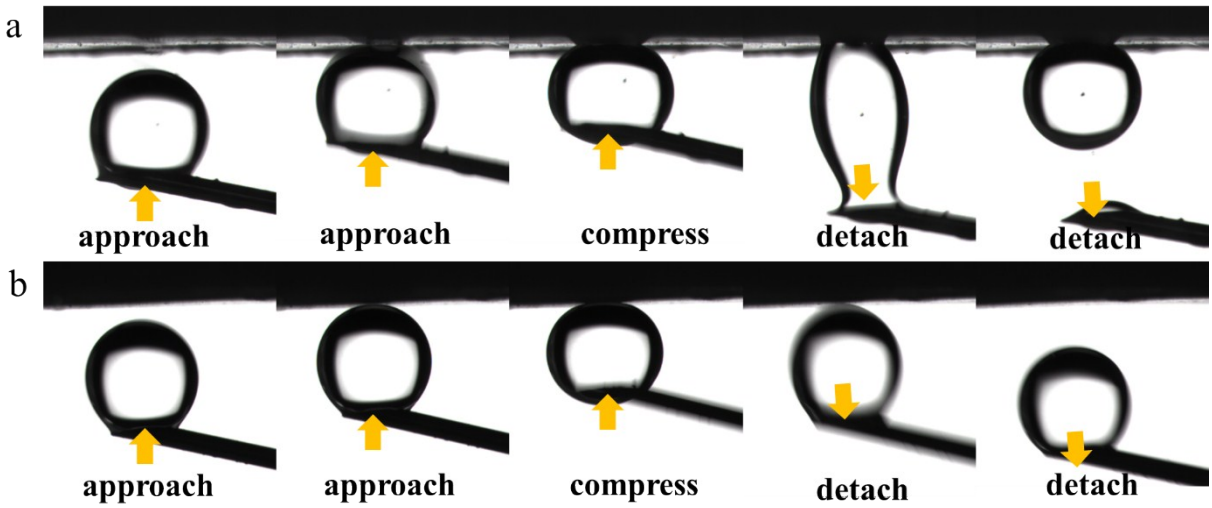

Fig. S16. Dynamic approach-compress-detach oil-adhesion process of (a) GO membrane and (b) GO/v-COF@GO membrane.

19. Characterization of surfactant-stabilized oil-in-water emulsion.

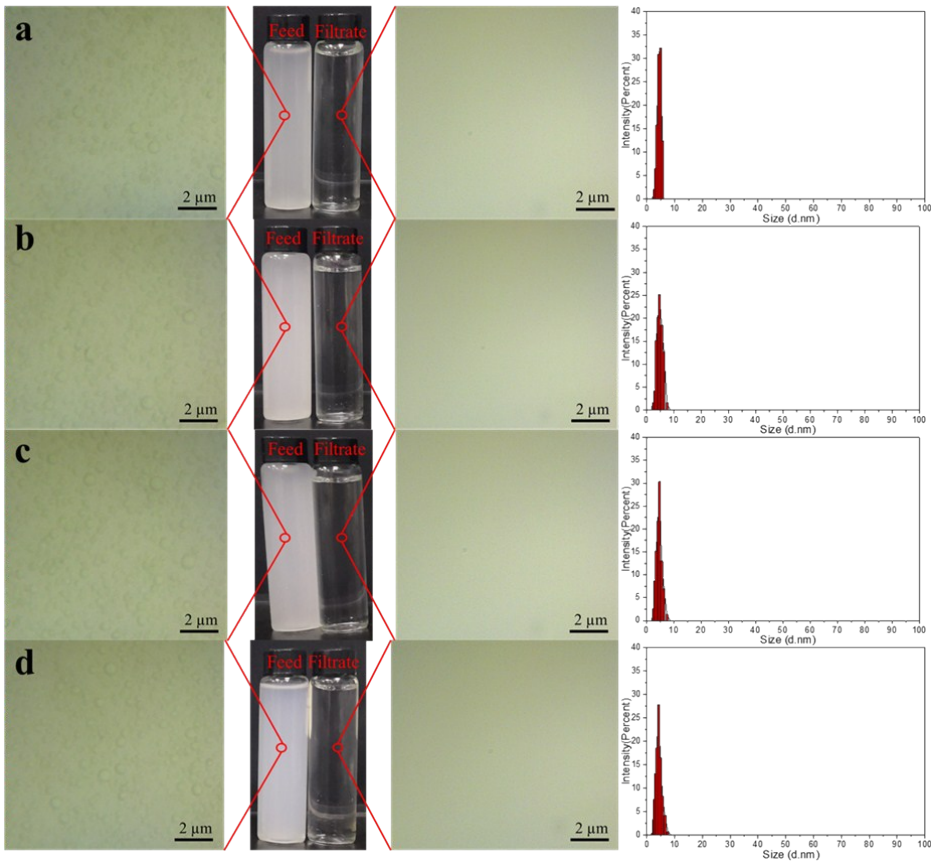

Fig. S17. The microscope pictures of the emulsion before and after separation, as well as the DLS data of the emulsion after separation, a) pump oil-in-water emulsion, b) silicone oil-in-water emulsion, c) soybean oil-in-water emulsion and d) hexadecane-in-water emulsion.

References

1. Joshi, R. K.; Carbone, P.; Wang, F. C.; Kravets, V. G.; Su, Y.; Grigorieva, I. V.; Wu, H. A.; Geim, A. K.; Nair, R. R. Precise and Ultrafast Molecular Sieving Through Graphene Oxide Membranes. Science 2014, 343, 752-754.

2. Wang, S.; Wu, Y.; Zhang, N.; He, G.; Xin, Q.; Wu, X.; Wu, H.; Cao, X.; Guiver, M. D.; Jiang, Z. A Highly Permeable Graphene Oxide Membrane with Fast and Selective Transport Nanochannels for Efficient Carbon Capture. Energ. Environ. Sci. 2016, 9, 3107-3112.

3. Chen, L.; Shi, G.; Shen, J.; Peng, B.; Zhang, B.; Wang, Y.; Bian, F.; Wang, J.; Li, D.; Qian, Z.; Xu, G.; Liu, G.; Zeng, J.; Zhang, L.; Yang, Y.; Zhou, G.; Wu, M.; Jin, W.; Li, J.; Fang, H. Ion Sieving in Graphene Oxide Membranes via Cationic Control of Interlayer Spacing. Nature 2017, 550, 415-418.

4. He, G.; Chang, C.; Xu, M.; Hu, S.; Li, L.; Zhao, J.; Li, Z.; Li, Z.; Yin, Y.; Gang, M.; Wu, H.; Yang, X.; Guiver, M. D.; Jiang, Z. Tunable Nanochannels along Graphene Oxide/Polymer Core-Shell Nanosheets to Enhance Proton Conductivity. Adv. Funct. Mater. 2015, 25, 7502-7511.

5. Lee, C. S.; Choi, M. k.; Hwang, Y. Y.; Kim, H.; Kim, M. K.; Lee, Y. J. Facilitated Water Transport through Graphene Oxide Membranes Functionalized with Aquaporin-Mimicking Peptides. Adv. Mater. 2018, 30, 1705944.

6. Xu, C.; Xu, Y.; Zhu, J. Photocatalytic Antifouling Graphene Oxide-Mediated Hierarchical Filtration Membranes with Potential Applications on Water Purification. ACS Appl. Mater. Interfaces 2014, 6, 16117-16123.

7. Huang, H.; Song, Z.; Wei, N.; Shi, L.; Mao, Y.; Ying, Y.; Sun, L.; Xu, Z.; Peng, X. Ultrafast Viscous Water Flow through Nanostrand-Channelled Graphene Oxide Membranes. Nat. Commun. 2013, 4, 2979.

8. Gao, S. J.; Qin, H.; Liu, P.; Jin, J. SWCNT-Intercalated GO Ultrathin Films for Ultrafast Separation of Molecules. J. Mater. Chem.A. 2015, 3, 6649-6654.

9. Liu, Y.; Su, Y.; Guan, J.; Cao, J.; Zhang, R.; He, M.; Gao, K.; Zhou, L.; Jiang, Z. 2D Heterostructure Membranes with Sunlight-Driven Self-Cleaning Ability for Highly Efficient Oil-Water Separation. Adv. Funct. Mater. 2018, 28, 1706545.